

Contents

Abbreviations	ii
1 Introduction	1
1.1 Smart Grid and Smart Building Automation	1
1.2 Load Monitoring	7
1.2.1 Conventional "Intrusive"	7
1.2.2 Non-intrusive Load monitoring	7
2 State of the Arts	10
2.1 Power disaggregation	10
2.2 Non-Intrusive Load Monitoring: Macroscopic	16
2.3 Non-Intrusive Load Monitoring: Microscopic	30

Abbreviations

WSN	Wireless sensor network
SG	Smart Grid
SBA	Smart Building Automation
HVAC	Heating, Ventilation and Air Conditioning
PIR	Passive Infrared Sensor
NIALM	Non-Intrusive Appliance Load Monitoring
RS	Reed Switch
NIOM	Non-Intrusive Occupancy Monitoring
DT	Decision Tree
DTW	Dynamic Time Warping
ANN	Artificial Neural Network
SOM	Self-Organizing Map
HMM	Hidden Markov Model
CFHSMM	Conditional Factorial Hidden Semi-Markov Model
MLE	Maximum Likelihood Estimation
FFT	Fast Fourier Transform
LAE	Least Absolute Error
NILM	Non-Intrusive Load Monitoring
EMS	Energy Management System
PLC	Power-Line Communication
DHW	Domestic Hot Water

Chapter 1

Introduction

1.1 Smart Grid and Smart Building Automation

Natural resource nowadays is the motivation for many researches on energy management in building and home. The energy management is not only the reduction of energy consumption but also the balance between it and the energy generation. Smart Grid (SG) and Smart Building Automation (SBA) are the approaches that have the main impact on energy saving problem.

The concept of SG is associated with the energy production side [1]. Concretely, the *grid* refers to the electric grid or a network of transmission lines, substations, transformers and other components that delivers the electricity from the power plants to the consumers. Meanwhile, the modern energy management techniques and communication infrastructure such as internet, wireless communication or Power-Line Communication (PLC) make the *grid* smart with the possibility of automated monitoring, computing, controlling without the humain intervention [2–5]. In addition, the purpose of SG also includes the integration of large-scale renewable energy systems such as wind power along the farms or solar power on the top of buildings in order to protect the environment and ecosystem, instead of using only the energy generated by the traditional power plants, e.g. hydropower, thermal power or nuclear power. Figure 1.1 illustrates an example of SG with the sensors along the transmission lines and the communication infrastructure.

In contrast, in SBA, the principle problem is how to reduce the energy consumption inside a house or a building. A smart building can be achieved by the generation and efficient

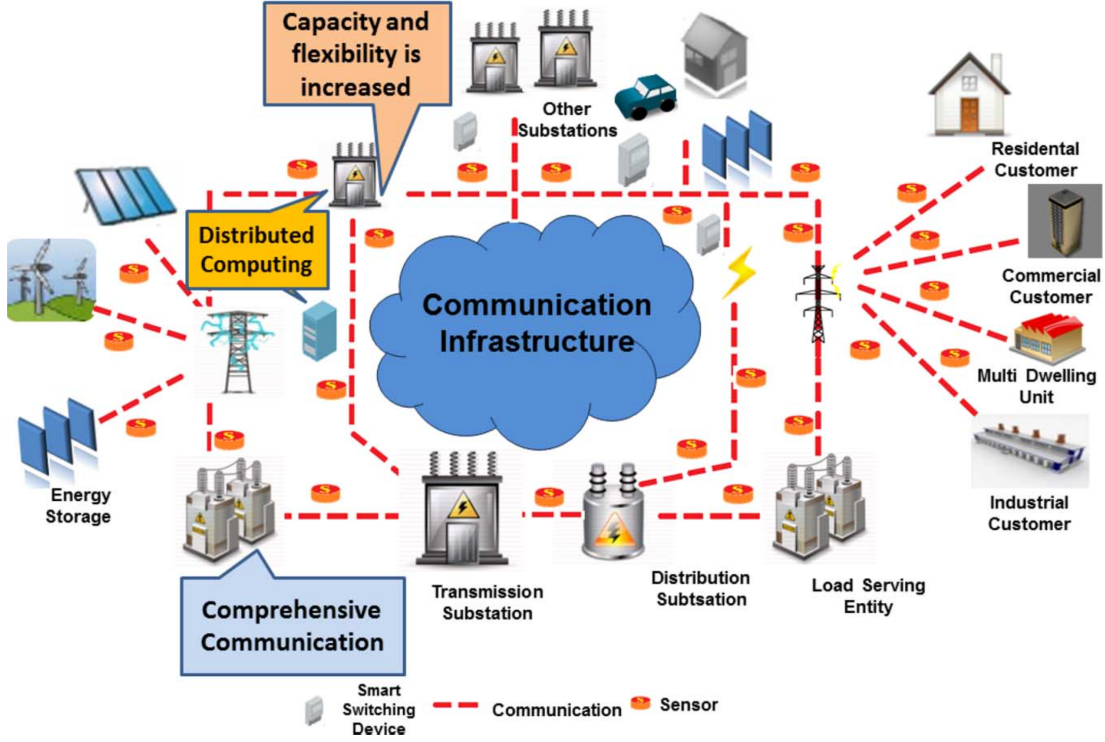


FIGURE 1.1: Smart Grid model [4].

usage of energy. The use modality of energy comes from the subsystems such as lighting system, office equipment, Heating, Ventilation and Air Conditioning (HVAC) system, etc. Therefore, the energy waste elimination effort can concentrate on these systems by sensing and automatically fluctuating their power to adapt to the environment condition. In a smart system, the human intervention must be restricted, the automation system automatically control the equipments through such a home Energy Management System (EMS). Similar to the SG, in SBA, the communication infrastructure plays an important role in exchanging the information among the components inside the EMS. That is the reason why PLC and Wireless Sensor Network (WSN) can be considered as potential solutions for environment monitoring and subsystem fluctuation, but the WSN is more attractive because of the flexibility and low cost. A typical smart building model is shown in Figure 1.2 while the main components of a SBA system applying wireless communication is represented in Figure 1.3. Several sensors capture the environment condition and send the report to the EMS center through wireless transceivers. The control center gets the information about the power consumption of the subsystems and fluctuates their power level to adapt to the environment variation.

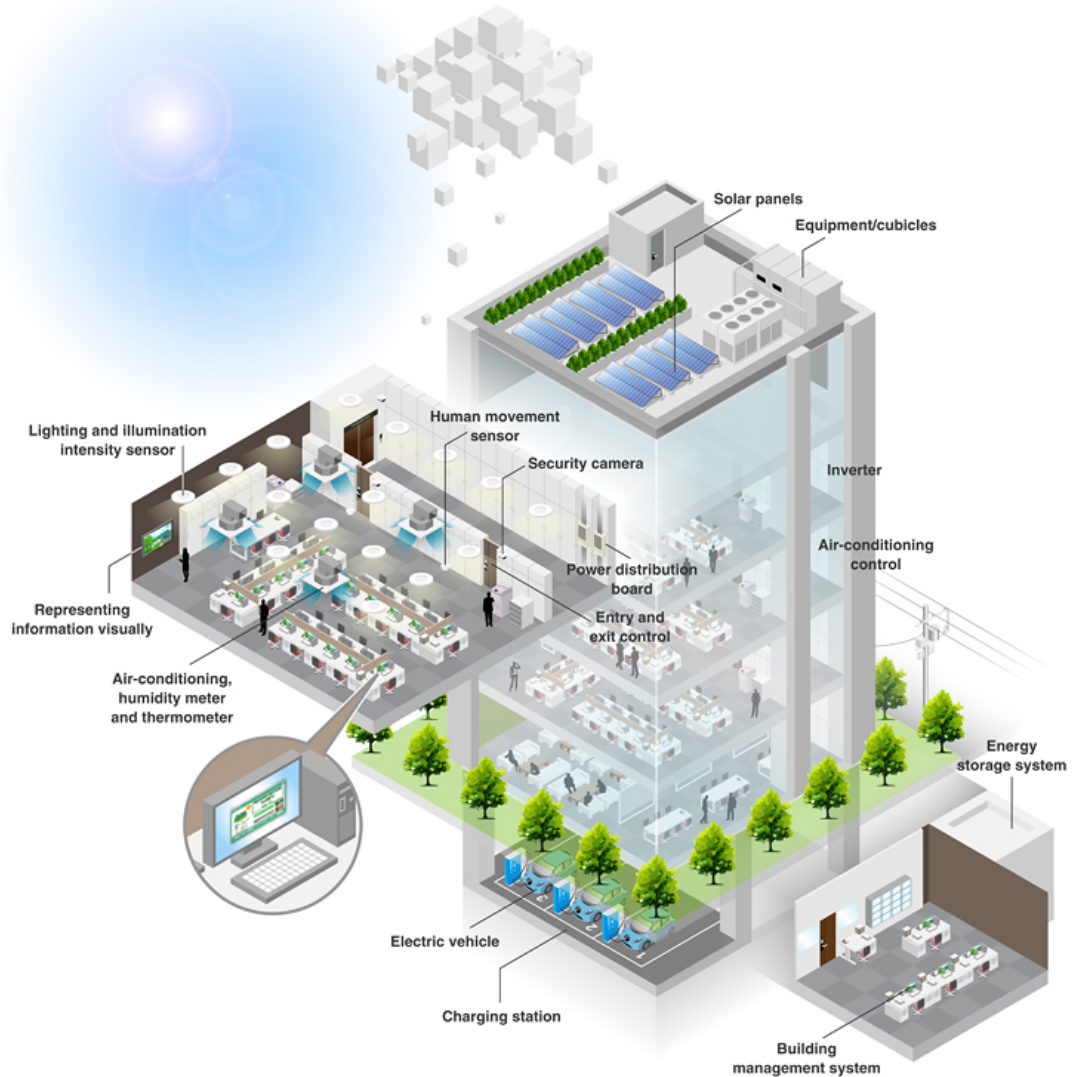


FIGURE 1.2: Smart Building Automation model [6].

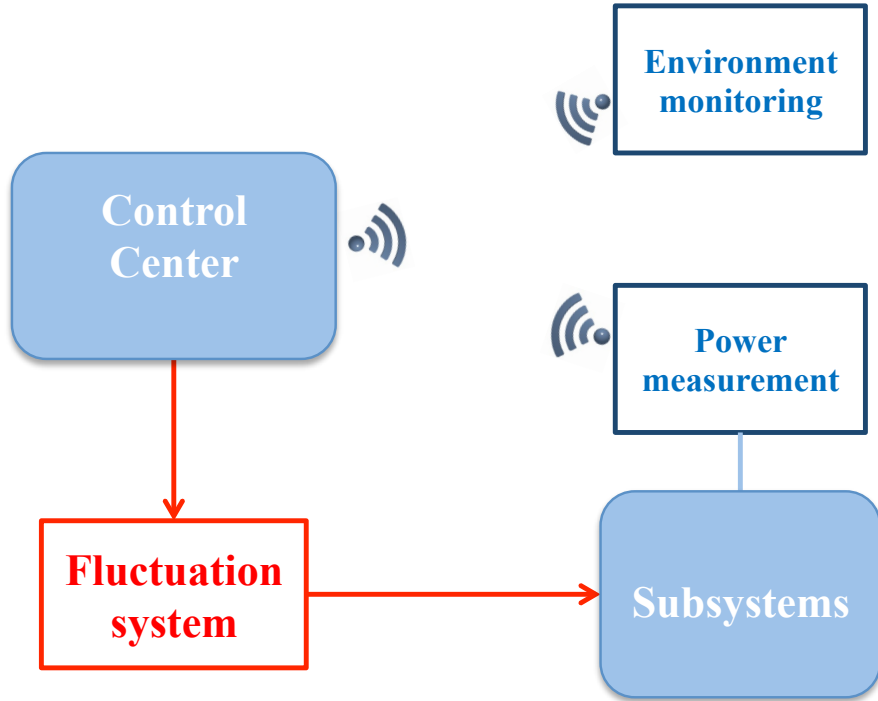


FIGURE 1.3: Principle components of a SBA system.

In this model, the environment can be the occupancy, light intensity, temperature, moisture or sound. Detecting and analyzing the environment conditions allows the control center to automatically regulate the equipment state to comfort the users, especially with the appliances requiring time to start up such as HVAC system. Last four types of environment above can be easily monitored by the corresponding sensors such as light sensors, temperature sensors, humidity sensors and microphones, respectively, while the occupancy detection is an interesting subject for many recent researches [7–10]. The occupancy can not only be directly detected by capturing the movement of the occupants by a Passive Infrared Sensor (PIR) or camera [7–9] but also indirectly detected by analyzing the events happening inside house or building, i.e. open door, change on the total power draw [11], abnormally increase of the CO₂ concentration [12].

In [7, 8], a couple of magnetic Reed Switch (RS) door sensor and PIR sensor is used to detect the occupancy of an office or room. Although PIR sensors are the most ubiquitous form for motion sensing, it is not enough for occupancy detection because people inside a room, especially inside an office, tend to maintain their posture when working in front of a computer, watching television or sleeping. To overcome this challenge, the combination with a RS door sensor, which can determine if the door is open or closed, is considered as a more feasible solution. If the door is open, the office is proposed as occupied, while

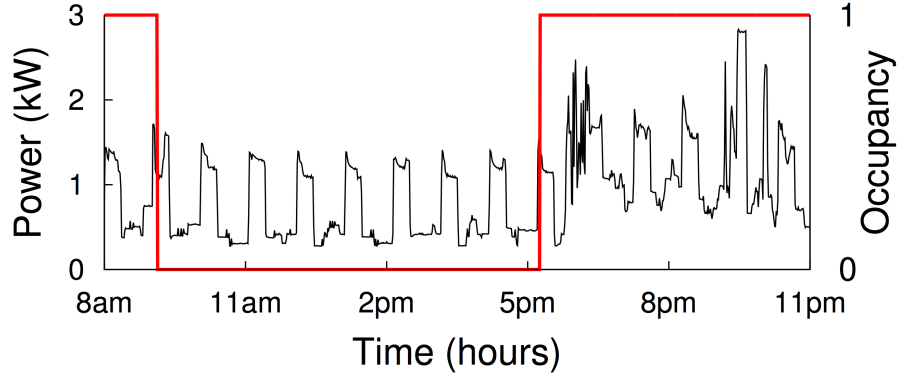


FIGURE 1.4: Variation on the power draw when the occupant turns on some devices [11]. The variation occurs on the average power, standard deviation and power range.

with the closed door, it is necessary to analyze the additional information from the PIR sensor before making the final decision. If the PIR sensor detects any movement, there is somebody inside. In contrast, the office is unoccupied. In comparison with the reference data coming from the direct observation and through camera, the detection accuracy of this method reaches to 96%. However, in some circumstances, this monitoring system is not efficient. Intuitively, if someone wants to make a phone call but he does not want to disturb the others outside, he can also close the door. During his call, he stays at his desk and does not make any movement. In this case, the PIR sensor cannot detect the occupancy and the detection system makes a mistake.

Meanwhile, in [11], the Non-Intrusive Occupancy Monitoring (NIOM) is introduced, in which an energy monitoring system was installed to gather the power usage at the individual branch circuits. The large changes in power, called events, are then extracted to analyze to detect the occupancy. As shown in Figure 1.4, the background load frequently appears and does not imply the occupancy. This load is derived from the presence of the appliances driven by an automated controller such as fridge or HVAC system. When having the presence of the occupants, their physical interactions with loads such as switching on the lamp, turning on the television, etc. will make change on the aggregate power usage. Obviously, the accuracy of NIOM strongly depends on the survey of background load due to the variation of this parameter according to the time of day and year such as day or night, spring or winter. For example, in the summer, only fridge operates, while during the winter, people tend to turn on the heater and that leads to the difference on the background load.

TABLE 1.1: NIOM accuracy (%) [11].

	True Positives	True Negatives	False Positives	False Negatives
Average power	53.50	24.84	0.54	21.12
Standard deviation	49.69	24.69	0.70	24.93
Power range	37.15	25.31	0.08	37.47
Combination	66.11	24.52	0.86	8.50

The authors of [11] also propose a simple threshold-based NIOM algorithm to detect the events by using three parameters of the aggregate power consumption: average power, standard deviation and power range. As illustrated in Figure 1.4, the average power usage significantly increases when home is occupied. At time t , the data points inside a power time-series window τ are averaged and compared with a predefined threshold $P_{average}$ to detect the presence of the occupancy. Both τ and $P_{average}$ must be jointly set. If τ is too small, $P_{average}$ should increase to be greater than the maximum average power over the window τ when the home is unoccupied to prevent the false alarm (no one is actually inside but the sensor detects the occupancy). In contrast, since τ becomes larger, $P_{average}$ should decrease to prevent the miss. For more efficiency, the average power is combined with the standard deviation because in some cases, the users can frequently toggle load on and off, the average power over the window τ at that time may be smaller than the $P_{average}$ threshold, but the standard deviation does rise above the predefined threshold P_{stddev} . Besides average power and standard deviation, the difference between the absolute minimum and absolute maximum power of τ consecutive data points or also called power range, can also be used to improve the efficiency of the system. If the average power and standard deviation do not overcome their thresholds, while the power range is larger than its threshold P_{range} , the occupancy will be taken into account. Table 1.1 resumes the accuracy of this algorithm when using three parameters separately and when combining them under summer condition and using nighttime-based threshold. Without the combination, the accuracy is under 80%, while the result can reach to over 90% if using simultaneously three metrics. The error essentially comes from the miss, i.e. the system cannot detect the occupancy while having some occupants inside the home.

Besides the environment monitoring, to form a smart building, the operating power of the equipments must have the possibility of automatically fluctuated to adapt to the environment variation. To do that, power sensing and metering play an important role.

1.2 Load Monitoring

1.2.1 Conventional "Intrusive"

Besides the environment monitoring sensors, the power measurement unit also requires a wireless protocol to communicate with the control center. The power measuring can be implemented by two ways: intrusive and non-intrusive. In intrusive approach, the measurement is implemented at each individual equipment, i.e. each appliance is connected to an power meter or an equivalent device. Each metering gives conclusion on only one monitored appliance. Meanwhile, the non-intrusive approach can detect and estimate the power consumption of all appliances on the monitored branch circuit with only one power meter installed on the main power line. Intuitively, non-intrusive approach helps to reduce the deployment cost but it requires a long period of observation to analyse the power characteristic of each appliance on the circuit.

In the conventional "Intrusive" branch, there are two kinds of metering including direct and indirect, as represented in Figure 1.5. The direct method obviously performs a high accuracy but having some disadvantages, i.e. it is not only necessary to interrupt the power source to install the meters, but the deployment and maintenance are also costly. Therefore, to limit the human intervention to the power supply as well as to reduce the cost, the indirect method is more interesting to study. In this method, some measurable signals emitted by the appliance when consuming energy will be sensed by some specific sensors. If the appliance has a limit number of internal states and each state demands a separable stable power level, the sensors, by detecting these states, can infer the corresponding consumed power. For example, to detect the state and estimate the power consumption of a television or a screen, a light sensor can be used or a refrigerator with four states is also detected by a couple of light sensor and acoustic sensor.

1.2.2 Non-intrusive Load monitoring

In contrast with the intrusive approach, the non-intrusive one uses only the power characteristics at the main power line to detect the events, determine the operating appliances and estimate the corresponding power consumption. Firstly, we assume N appliances supervised by a unique power meter. Each appliance $i \in \{1, \dots, N\}$ can operate at one

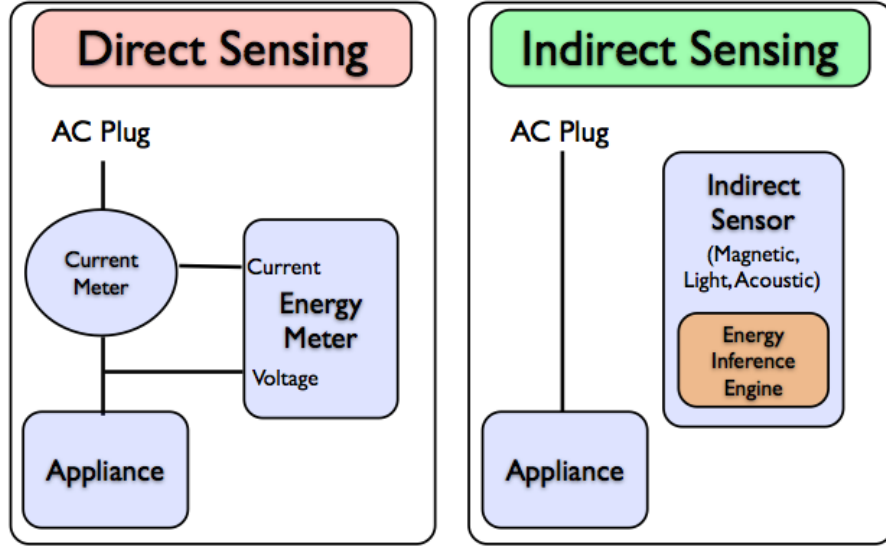


FIGURE 1.5: Direct and indirect power measurement [13].

state j of M_i modes, that consumes an amount of power of w_{ij} , $j \in \{1, \dots, M_i\}$. Denote $s_{ij}(t)$ as the Boolean indicator of $j - th$ state of $i - th$ appliance at time t :

$$s_{ij}(t) = \begin{cases} 1 & \text{if appliance is on,} \\ 0 & \text{if appliance is off.} \end{cases}$$

The aggregate power consumption can be represented as follows:

$$x(t) = \sum_{i=1}^N \sum_{j=1}^{M_i} s_{ij}(t) \times w_{ij} + e(t), \quad (1.1)$$

where $e(t)$ is a small noise or error term. From this model, the indicator vector s can be determined by solving the minimization problem:

$$\hat{s}(t) = \arg \min_s \| x(t) - \sum_{i=1}^N \sum_{j=1}^{M_i} s_{ij}(t) \times w_{ij} \| . \quad (1.2)$$

This problem is computationally intractable, it is impractical to exactly solve by exhaustive techniques unless n is small. Instead, the heuristic algorithms might be considered. There are three principles for any NILM method, including:

- Select and mathematically characterize the specific appliance features or signatures;

- Require the hardware installation to detect those features;
- Construct a mathematical algorithm to detect those features from the overall signal.

The selection of features and signatures depends on the hardware frequency of the meter. They can be divided into 2 small groups: low frequency and high frequency.

The related works of load monitoring will be presented in the next section.

Chapter 2

State of the Arts

2.1 Power disaggregation

The naive and costly method to measure the power consumption of the appliances is to connect each individual one to a power meter. Apparently, this approach is not able to deploy in real condition because of high cost and technical intervention on the power supply. Therefore, Kim et al. [13] propose a system called ViridiScope to replace a part of power meters by indirect sensing comprising of a set of sensors which can detect the environment around the monitored devices and imply their operation state. In ViridiScope, the appliances with stable power demand can be monitored by the indirect sensors such as light, acoustic sensors, while the variable loads can be measured by a magnetometer or a direct AC meter. Another AC meter is also installed at the main power line to measure the aggregate power usage of the system. With magnetic sensor, the magnetic field changes at 100 Hz and the signal $s_i(t)$ is formed from the sample standard deviation over an one second sliding window. The power consumption of i -th appliance correlating to this signal is defined as follows:

$$x_i(t) = \alpha_i s_i(t) + \beta_i, \quad (2.1)$$

where α_i, β_i are the calibration parameters. The contactless electromagnetic field sensor is also designed to sense the appliance state transitions within close proximity through the variations in electric and magnetic field, as introduced in [14] and illustrated in Figure 2.1. The electric field is created from the difference in voltages, i.e. a strong

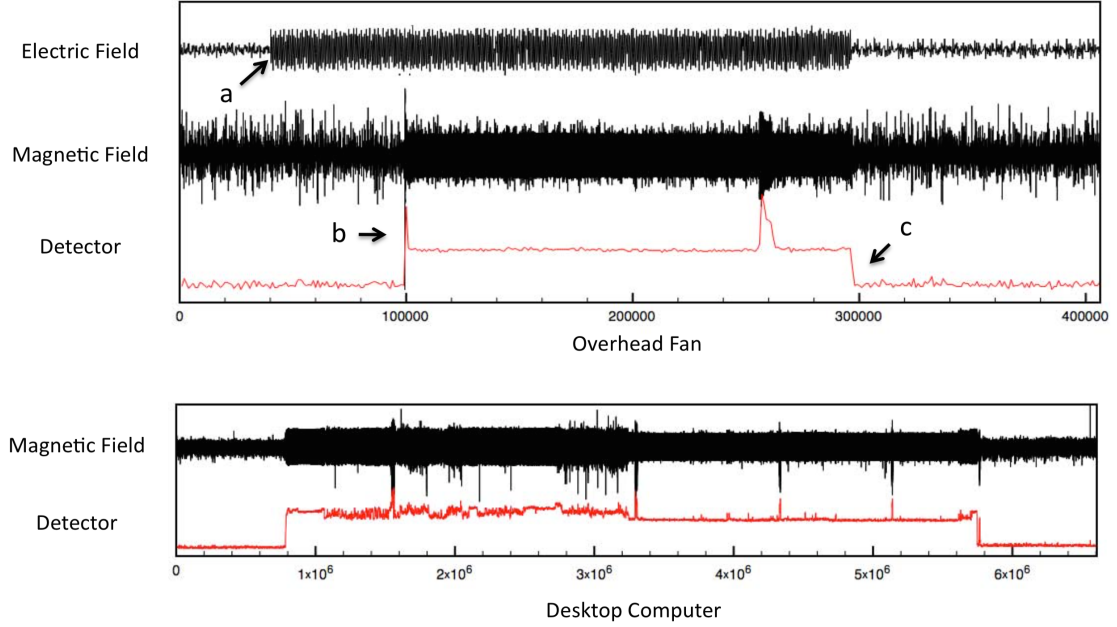


FIGURE 2.1: Electromagnetic field event detector waveform. Top: Overhead fan is powered up at point (a), switched on at point (b) and switched off at point (c). Bottom: Variations in magnetic field near by the desktop computer [14].

electric field may be generated even when the appliance does not draw current, while the variation of the magnetic field corresponds to the change of the power consumption. Therefore, the electric field can be used to determine if the appliance is powered or not.

Meanwhile, with the appliances having a limit number of power states, the power consumption can be estimated by detecting the internal state. This detection can be implemented thanks to light sensor and/or acoustic sensor. Let $s_{ij}(t)$ be an indicator function indicating the j -th internal state of the i -th appliance. The power consumption is estimated by the following equation:

$$x_i(t) = \sum_{j=1}^{M_i} w_{ij} s_{ij}(t), \quad (2.2)$$

where M_i is the number of internal states of the i -th appliance, w_{ij} is the average power of the j -th state and $s_{ij}(t)$ is a Boolean indicator function that indicates the on/off state of the j -th state of i -th appliance.

Additionally, some appliances can be supervised by a direct meter, so their power consumption can be directly read from the meter. That means:

$$x_i(t) = \tilde{x}_i(t), \quad (2.3)$$

where $\tilde{x}_i(t)$ is the data read from the direct meter.

Besides the appliances supervised by one or a group of sensors, ViridiScope also considers the uninstrumented appliances, which are not supervised by any sensor. Denote w_i as the average power consumption of these appliances, the power consumption is as follows:

$$x_i(t) = w_i s_i(t), \quad (2.4)$$

where $s_i(t)$ is the indicator function indicating that the uninstrumented appliances are present in the configuration or not. Obviously, the total power consumption of a household is the sum of the power consumption of all appliances, denoted as N . Therefore, an explicit numerical optimization problem is formulated from equations (2.1), (2.2), (2.3), (2.4) as follows:

$$\min \| x(t) - \sum_{i=1}^N x_i(t) \|$$

where

$$x_i(t) = \begin{cases} \alpha_i s_i(t) + \beta_i : \text{magnetometers} \\ \sum_{j=1}^{M_i} w_{ij} s_{ij}(t) : \text{light/acoustic sensors} \\ w_i s_i(t) : \text{un-instrumented} \\ \tilde{x}_i(t) : \text{direct meter input}, \end{cases} \quad (2.5)$$

where $\| . \|$ denotes the $l1$ -norm or Least Absolute Value Regression which solves for the median value, and α , β , w_i , w_{ij} are the control variables, which need to be found as solution for the $l1$ -norm minimization. The $l1$ -norm is used in the ViridiScope system instead of $l2$ -norm, Least Mean Square Regression, because the $l2$ -norm solves for the average value and the median operator is more robust to outliers than the mean operator. By solving this minimization problem, the power usage of each individual appliance is estimated as represented in Figure 2.2.

The accuracy of ViridiScope system is larger than 90%, however, there are some limitations. In the current implementation, the uninstrumented devices are assumed to consume a constant power, while this power can vary depending on the type of devices. Additionally, large amount of sensors is necessary for deployment to reduce the number of uninstrumented devices and increase the accuracy of the system.

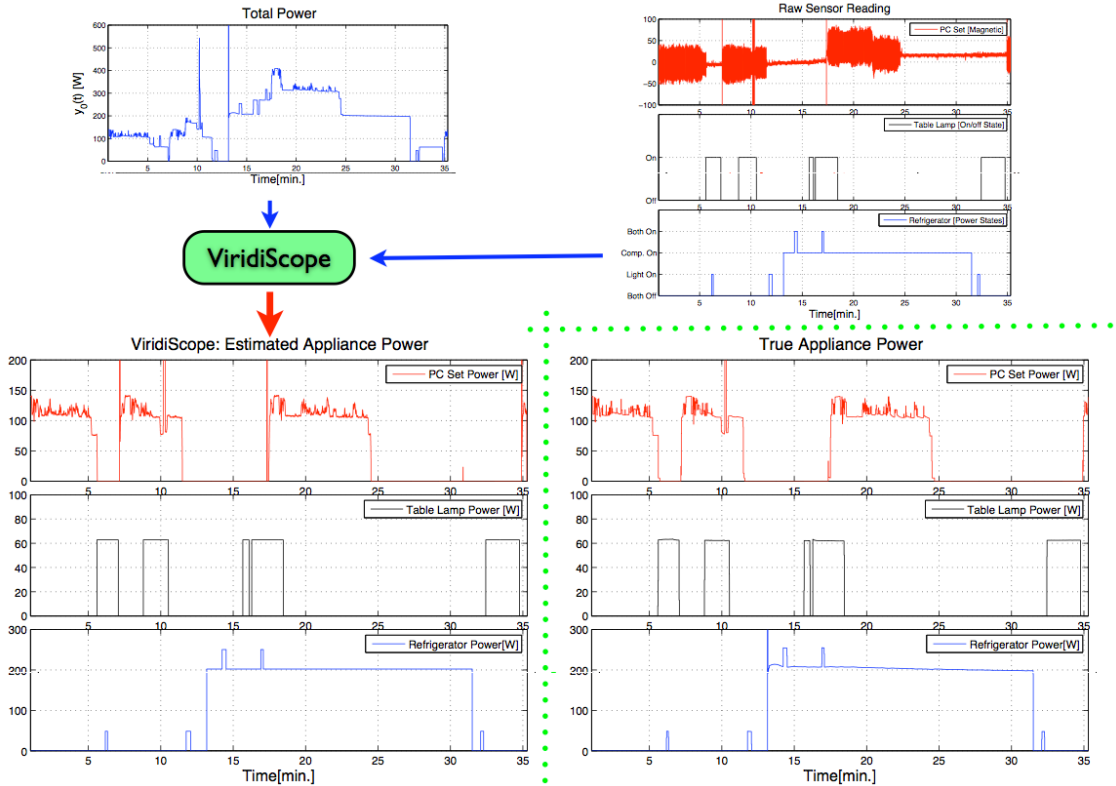


FIGURE 2.2: The ViridiScope system takes the total power consumption, magnetic field and internal power states information to estimate the power usage of each individual appliance by solving the l_1 -norm minimization problem [13].

Similar to ViridiScope, in [15, 16], Jung and Savides propose to use only binary sensors to detect the ON/OFF state of the energy consumers inside the building and then disaggregate the total power consumption to each individual appliance. The fundamental difference between this method and ViridiScope is to use the binary sensors providing the ON/OFF state instead of raw data as in ViridiScope. In addition, because only binary sensors are used, the power consumption of the variable loads or multi-state devices cannot be accurately estimated. All appliances are assumed to consume a stable power level during their ON state. Therefore, to increase the accuracy, the observation time interval used to estimate the power usage of each appliance needs to be short enough. Besides, if the ON/OFF sequences of more than two appliances are synchronized, the panel power cannot be disaggregated. In this case, to reach the desired accuracy, some additional power meters are placed to the necessary electrical outlets, as illustrated in Figure 2.3 where the dark node denotes the presence of a power meter. In this example, because the ON/OFF sequences of appliances x_2 and x_5 are synchronized, their power is difficult to estimate if they are connected to the same power meter as in the left topology or in topology 2. In contrast, in topology 1, appliances x_2 and x_5 are connected to different

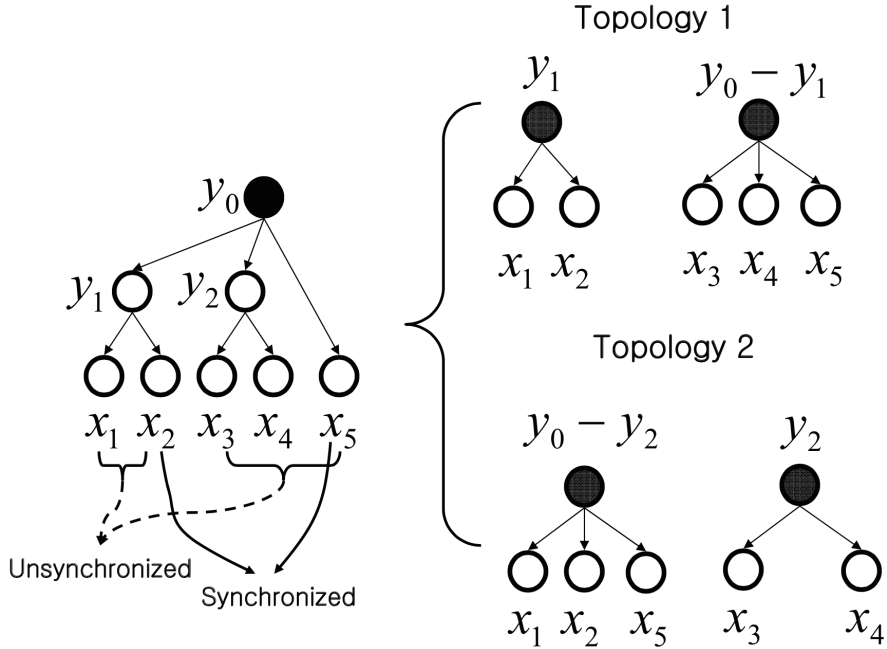


FIGURE 2.3: Illustrative example of power meter topology. The left topology uses only one power meters (dark node) at the main power supply while topology 1 and 2 use two additional power meters at the electrical outlets [15].

meters, a better performance of disaggregation can be achieved.

However, a shortcoming in the research of Jung and his colleague is to ignore the presence of the *ghost power* coming from the uninstrumented appliances not monitored by any sensor. Beckel et al. [17] found this drawback when applying this method to the REDD public dataset [18], which is available at <http://redd.csail.mit.edu>. The dataset contains the electricity consumption measurement from six households in the USA from April to May 2011. The REDD dataset provides the data measured from two phases of each house and the power consumption of several individual circuits. Because there are many uninstrumented appliances in each house, the method proposed in [15] leads to low performance of disaggregation. To solve this problem, the authors of [17] assume to add an "always-on" *virtual ghost power consumer* to the set of monitored devices. They also assume that all appliances are perfectly monitored by the binary sensors and the ON/OFF events are extracted from the electricity consumption of the individual circuits. By this way, the disaggregation algorithm can improve its performance defined by the difference between the estimated power and real power consumption of each appliance.

Another technique applied to disaggregate the power consumption to each individual appliance is sparse coding [19]. In this method, the power signal is sampled every 15

minutes and the training data of each appliance is contained in matrix $W_i \in \mathbb{R}^{T \times m}$ in which each column corresponding to the data of one week. The aggregate power consumption is then $W = \sum_{i=1}^N W_i$. Applying the sparse coding, the following approximation is considered:

$$W_i = B_i \times A_i, \quad (2.6)$$

where $B_i \in \mathbb{R}^{T \times n}$ contains n basis functions or *dictionary*, and $A_i \in \mathbb{R}^{n \times m}$ contains the *activations* of basis functions. In the training period, the values of B_i and A_i are estimated by the following minimization:

$$\min_{A_i \geq 0, B_i \geq 0} \frac{1}{2} \| W_i - B_i \times A_i \|_F^2 + \lambda \sum_{p,q} (A_i)_{pq} \text{ subject to } \| b_i^{(j)} \|_2 \leq 1, j = 1, \dots, n, \quad (2.7)$$

where $\| Y \|_F \equiv (\sum_{p,q} Y_{pq})^{1/2}$ is the Frobenius norm, and $\| y \|_2 \equiv (\sum_p y_p^2)^{1/2}$ is the l_2 -norm. Whenever the algorithm is applied to disaggregate a new set of data $X \in \mathbb{R}^{T \times m'}$, the value of A_i is recalculated as follows:

$$\begin{aligned} \hat{A}_{1:N} &= \arg \min_{A_{1:N} \geq 0} \| X - [B_1 \cdots B_N] \begin{bmatrix} A_1 \\ \vdots \\ A_N \end{bmatrix} \|_F^2 + \lambda \sum_{i,p,q} (A_i)_{pq} \\ &\equiv \arg \min_{A_{1:N} \geq 0} F(X, B_{1:N}, A_{1:N}). \end{aligned} \quad (2.8)$$

Finally, the power is disaggregated to each individual appliance by the following equation:

$$\hat{X}_i = B_i \times \hat{A}_i. \quad (2.9)$$

However, fixing the coefficients B_i will reduce the accuracy of the algorithm. Instead, an iterative method for discriminative disaggregation, in which each coefficient of A_i and B_i is trained until convergent, is introduced in Algorithm 1.

It is not difficult to realize that the sparse coding based disaggregation algorithm needs an excessive training data set. Additionally, this method is only used in off-line mode and cannot detect the operating appliances instantaneously. Meanwhile, with the sensor-based disaggregation algorithms in [13, 15, 16], although the direct power meters are replaced by the indirect sensors to reduce the deployment cost, they still needs a large

Algorithm 1 Discriminatative disaggregation sparse coding [19].

Input: data points for each individual source $W_i \in \mathbb{R}^{T \times m}$, $i = 1, \dots, N$, regularization parameter $\lambda \in \mathbb{R}_+$, gradient step size $\alpha \in \mathbb{R}_+$.

Sparse coding pre-training:

1. Initialize B_i and A_i with positive values and scale columns of B_i such that $\|b_i^{(j)}\|_2 = 1$.
2. For each $i = 1, \dots, N$, iterate until convergence:
 - (a) $A_i \leftarrow \arg \min_{A \geq 0} \|W_i - B_i \times A_i\|_F^2 + \lambda \sum_{p,q} A_{pq}$
 - (b) $B_i \leftarrow \arg \min_{B \geq 0, \|b_i^{(j)}\|_2 \leq 1} \|W_i - B \times A_i\|_F^2$.

Discriminative disaggregation training:

3. Set $A_{1:N}^* \leftarrow A_{1:N}$, $\tilde{B}_{1:N} \leftarrow B_{1:N}$.
4. Iterate until convergence:
 - (a) $\hat{A}_{1:N} \leftarrow \arg \min_{A_{1:N} \geq 0} F(X, \tilde{B}_{1:N}, A_{1:N})$
 - (b) $\tilde{B} \leftarrow \left[\tilde{B} - \alpha \left((X - \tilde{B} \times \hat{A}) \hat{A}^T - (X - \tilde{B} \times A^*) (A^*)^T \right) \right]_+$
 - For all i, j , $b_i^j \leftarrow b_i^j / \|b_i^{(j)}\|_2$.

Given aggregated test examples X' :

5. $\hat{A}'_{1:N} \leftarrow \arg \min_{A_{1:N} \geq 0} F(X', \tilde{B}_{1:N}, A_{1:N})$
 6. Predict $\hat{X}'_i = B_i \times \hat{A}'_i$.
-

amount of sensors as well as the technical intervention. To radically decrease the implementation cost, the presence of sensors needs to be eliminated and the operating state of the appliances needs to be detected based only on the aggregate power measured at the main entry of the electricity. This approach is called Non-Intrusive Load Monitoring (NILM) and firstly proposed by G.Hart [20] in the early 1990s. The researches on NILM can be divided into two main approaches: low frequency hardware based (macroscopic) and high frequency hardware based (microscopic) [21].

2.2 Non-Intrusive Load Monitoring: Macroscopic

With low frequency hardware based approach, the promising signatures have a relation with the real and reactive power such as average power during the steady state or step-change when switching on/off or changing the power state of an appliance. The step-change analysis method was firstly introduced by G.Hart [20]. In this method, the changes on the power draw, as shown in Figure 2.4, are detected by an edge detector. In Figure 2.5, the transient-passing step-change detector segments the power draw into periods in which the power is steady and periods in which it changes. A steady period is defined as a set of consecutive instants in which the power does not vary more than a threshold. The samples in a steady period are then averaged and the difference between

two consecutive steady periods is called step-size. Let $p(t_k)$ be the measured power at time t_k and denote $p(t_k) = p(kT) = p(k)$, where $T = t_k - t_{k-1}$ is the sampling interval. $p(k)$ is then expressed as:

$$p(k) = \sum_{i=1}^N p_i(k) + n(k), \quad (2.10)$$

where $p_i(k) \geq 0$ and $n(k)$ are the power load of appliance i and noise, respectively, at time instant kT . An event occurs when an appliance changes its state, i.e. $|p_i(k) - p_i(k-1)| \geq W$, with the threshold W . Therefore, the edge detector compares the value of $|p(k) - p(k-1)|$ with W to detect the events. An event is determined as started at time l_s and ended at time l_e if:

$$|[p(l_s) - p(l_s - 1)] + [p(l_e) - p(l_e - 1)]| \leq C, \quad (2.11)$$

where C is a practical estimated parameter. A cluster analysis maps the detected step-changes to a two-dimensional signature space of real and reactive power. The rising and falling edges of an event are then paired and compared with the existing clusters from the training procedure to identify the loads using maximum likelihood algorithm. An example of the position of some specific devices on the P-Q plane in home are represented in Figure 2.6. Besides, to reduce the effect of the voltage fluctuations, the following normalization is also proposed:

$$x_{norm}(t) = \left[\frac{120}{V(t)} \right]^2 \times x(t), \quad (2.12)$$

where V is the voltage, x the power consumption and 120 V corresponds to the nominal voltage in USA distribution system.

The edge detection based method proposed by G. Hart is suitable to detect and identify the on/off events on the power draw, however, it still exists some limitations. The first limitation is that it is only applied to the stable load appliances. The variable loads such as computers, whose power consumption depends on the running tasks, cannot be detected. The second drawback of the edge detector is the ambiguity when having the confusion on the power demand of more than two devices. To improve the detection accuracy, some later researches are developed from this method and apply other additional features. In [22], a median filter is applied to remove the meaningless abrupt peaks in the raw signal and therefore, the step-change detection becomes more accurate. Meanwhile

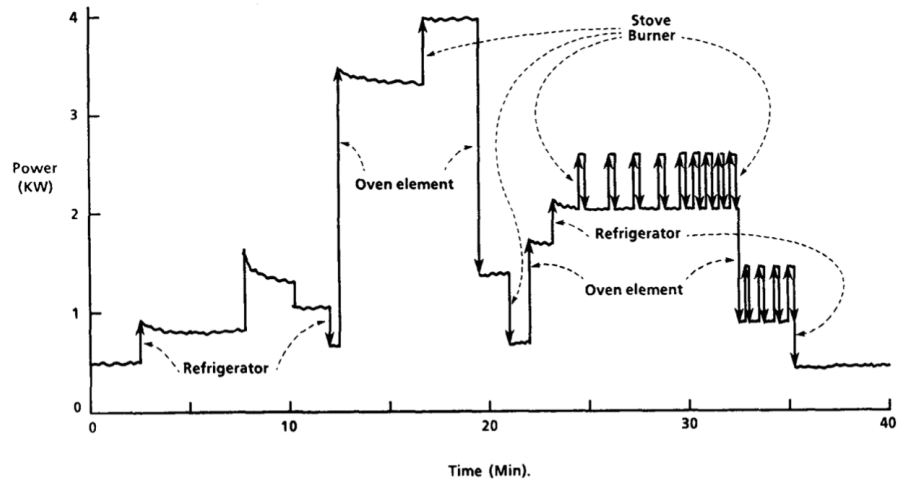


FIGURE 2.4: Power *vs.* time plot shows step changes due to individual appliance events [20].

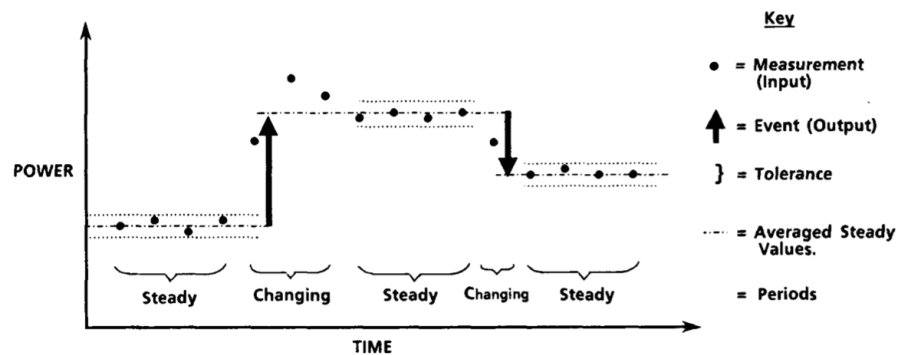


FIGURE 2.5: Detecting step-changes [20].

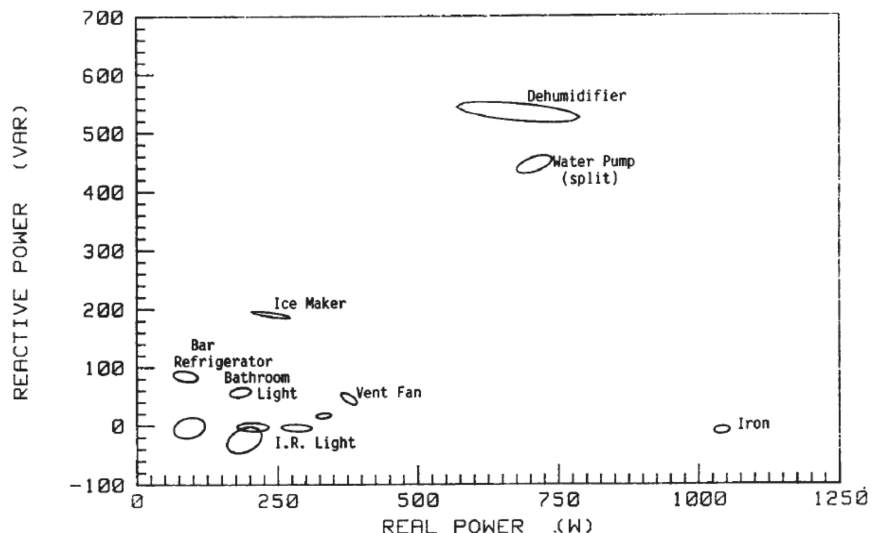


FIGURE 2.6: Clusters of some appliances on P-Q plane [20].

in [23], edges and slopes, defined as the slow changing variations after an initial upward spike in power when switching on an appliance, are simultaneously used as a feature to detect the appliances having variations in power consumption before reaching the steady state such as heat pumps, dish washers, fridges, ect.

Similar to [20], the authors of [24] also try to detect and pair the rising and falling edges of an event and construct a Decision Tree (DT) algorithm, clarified in Algorithm 2, to identify the appliance creating that event. However, for one individual appliance, only edges having maximum and minimum values are kept instead of all possible edges. Thus, only $2N$ values are saved in the library.

Algorithm 2 DT classification procedure [24].

```

1: function DTPREDICT( $T$ ,  $DTmodel$ )
2:    $node = root$ 
3:   repeat
4:     if  $T < V(node)$  then
5:        $node = left_{child}$ 
6:     else
7:        $node = right_{child}$ 
8:     end if
9:   end if
10:  until  $node$  is a leaf in  $DTmodel$ 
11:   $class = \text{Appliance}(node)$ 
12:  return  $class$ 
13: end function
14: end function
```

In this algorithm, the decision tree includes a *root*, several *nodes* and *leaves* relating to the known or undefined appliances. At each node, a split point value $V(node)$ calculated from the training period is used to decide the *child* node, i.e. left or right. The splitting procedure iterates until any *leaf* node is reached, i.e. the event is matched to an individual appliance.

Beside DT, another so-called Dynamic Time Warping (DTW) algorithm is also presented in [24]. Different from the DT algorithm, with DTW, all values of an event from the rising edge to the falling edge are kept in a vector instead of only the start and end points. Because the length of the events are varied, the DTW-based method is proposed to use a pattern matching procedure via dynamic programming. When an event is detected, the accumulated distances between it and all patterns in library given from the training

period are calculated, as described in Algorithm 3. The appliance having the pattern giving the smallest distance to the event will be identified.

Algorithm 3 DTW pattern matching: Find distance between two vector with different lengths [24].

```

1: function DTW( $p, q$ )
2:    $n = \text{length}(p)$ 
3:    $m = \text{length}(q)$ 
4:    $D(0, 0) = 0, D(i, 0) = D(0, i) = \infty$ 
5:   for  $i = 1, \dots, n$  do
6:     for  $j = 1, \dots, m$  do
7:        $d(i, j) = |p(i) - q(j)|$ 
8:        $D(i, j) = d(i, j) + \min \{D(i - 1, j), D(i - 1, j - 1), D(i, j - 1)\}$ 
9:     end for
10:    end for
11:   end for
12:   end for
13:   Output  $D(n, m)$ 
14: end function
15: end function
```

To test the algorithms, both DT and DTW are applied to identify the events from REDD dataset. Three evaluation metrics are used to evaluate their performance, including precision (PR), recall (RC) and F-measure (F_M) [25], defined as:

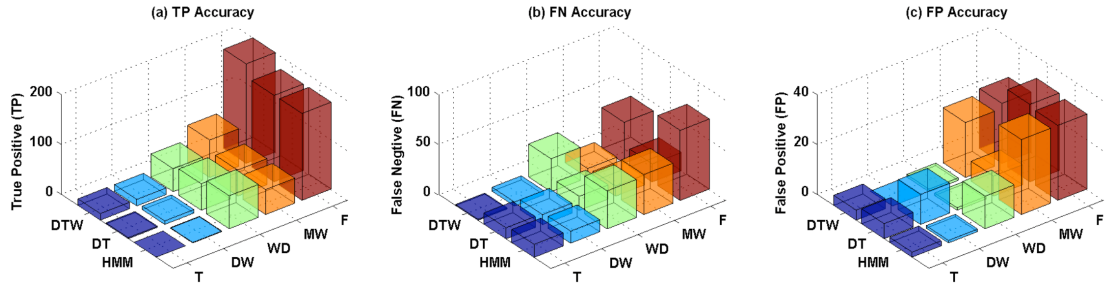
$$\begin{aligned} PR &= \frac{TP}{TP + FP} \\ RC &= \frac{TP}{TP + FN} \\ F_M &= \frac{2 \times (PR + RC)}{PR + RC}, \end{aligned}$$

where TP , FP , FN are the number of true positives, false positives and false negatives, respectively. A true positive means an event is correctly detected, while a false positive is taken into account if a non-event is wrong detected as event, and a false negative appears when an event is detected as non-event. The results when applying the DT and DTW algorithms to the House 1, House 2 and House 6 of REDD dataset are presented in Table 2.1 and compared with the Hidden Markov Model (HMM) based method. The values of TP , FN , FP of the three methods related to some specific appliances in House 1 are also illustrated in Figure 2.7.

In another research, Batra and his colleagues propose to apply the edge detection based algorithm in [20] to the REDD dataset, but divide the aggregate power into two main

TABLE 2.1: Comparison between the three methods using REDD dataset [24].

	PR(%)			RC(%)			FM(%)		
	DTW	DT	HMM	DTW	DT	HMM	DTW	DT	HMM
House									
House 1	85.01	78.09	79.29	79.72	78.09	62.72	82.28	78.09	70.04
House 2	89.86	80.80	51.80	84.39	82.03	62.79	87.04	81.41	56.77
House 6	98.86	76.14	99.30	81.22	75.76	74.74	89.17	75.94	85.29

FIGURE 2.7: TP , FN and FP for the three methods related to some specific appliances in House 1 of REDD dataset. T is toaster, DW is dishwasher, WD is washer dryer, MW is microwave and F is refrigerator [24].

phases [26]. This division helps to reduce the state space from K^N down to K^{N_p} where K , N , N_p are the number of states of each appliance, number of devices in whole house and number of devices connected to phase p , respectively. With the buildings using two or three phases of electricity like in REDD dataset, this method can significantly improve the computation complexity by reducing the size of state space.

To improve the quality of edge detection, in [27], the aggregate power sampled at 16s period goes through a preprocessing block to filter the signal, remove the fluctuations and useless spikes, which are very short and followed by a relatively long period of stable demand, before applying the recognition algorithm. In the power disaggregation procedure shown in Figure 2.8, the sample statistics block uses the training data to extract the characteristics of the operating appliances. After preprocessing the data, in the recognition block, an edge detector like in [20] is applied to detect the step-changes and compare with the operating range of the appliances in the library to identify the events. Besides, this algorithm uses some additional checking subroutines to improve the performance. The first one is the *average duration checking* (or *maximum duration checking* with refrigerator and water heater). Because the monitored appliances in this research including the water heater, baseboard heater, washing machine and refrigerator only operate during a certain average duration (maximum duration with refrigerator

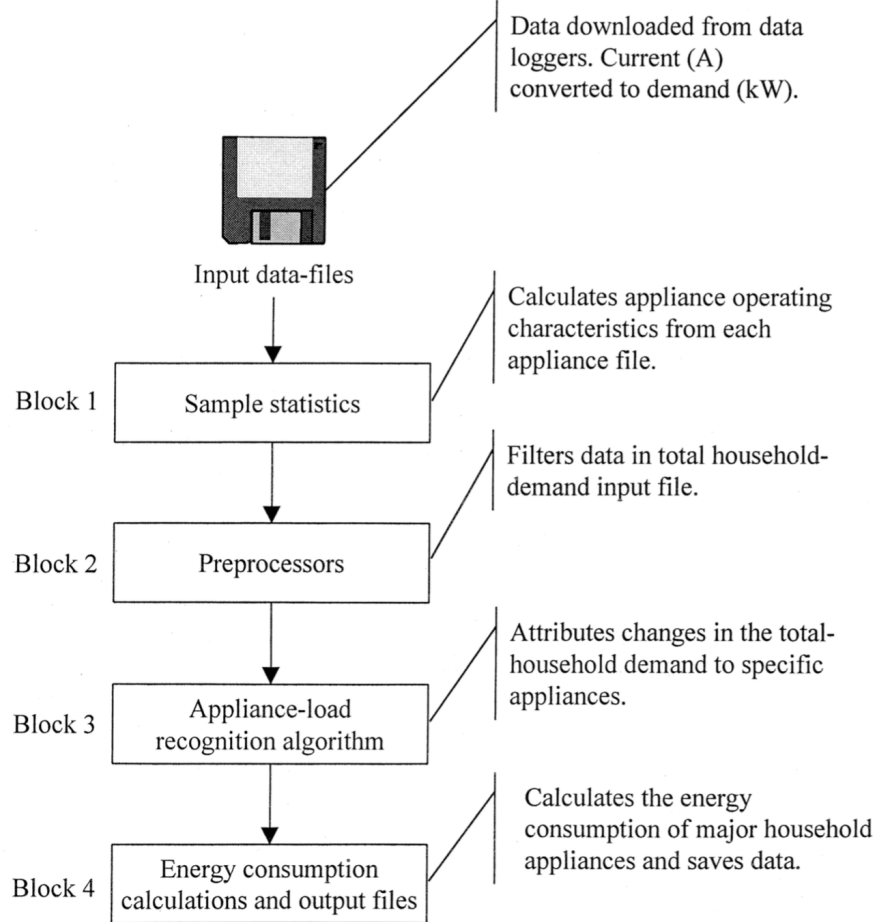


FIGURE 2.8: Load disaggregation procedure [27].

and water heater), if any appliance is marked as ON longer than its average duration, its state will be automatically changed to OFF. Meanwhile, the second subroutine called *zero demand checking* will reset the state of all appliances to OFF if the total power decreases to zero. In the third one, if an OFF signal matches with an appliance range whose previous state is not ON, a program will backtrack to the previous events and apply some wider criteria to determine the switched-on appliance. As evaluated in [27], with this procedure, the achieved error is less than 10% in most evaluation scenarios. However, it exists some limitations, e.g. a long preprocessing before recognizing the appliances is required or only appliances operating in a limit duration can be applied.

Similarly, to identify the large appliances such as water heaters and refrigerators from the total demand profile, Farinaccio and Zmeureanu [28] also propose a so-called *top-bottom rule-based* algorithm. In this algorithm, the decision rules are applied to the features extracted from the real power data at 16s sampling rate to recognize the corresponding appliances. These features are individually chosen depending on the type of appliances

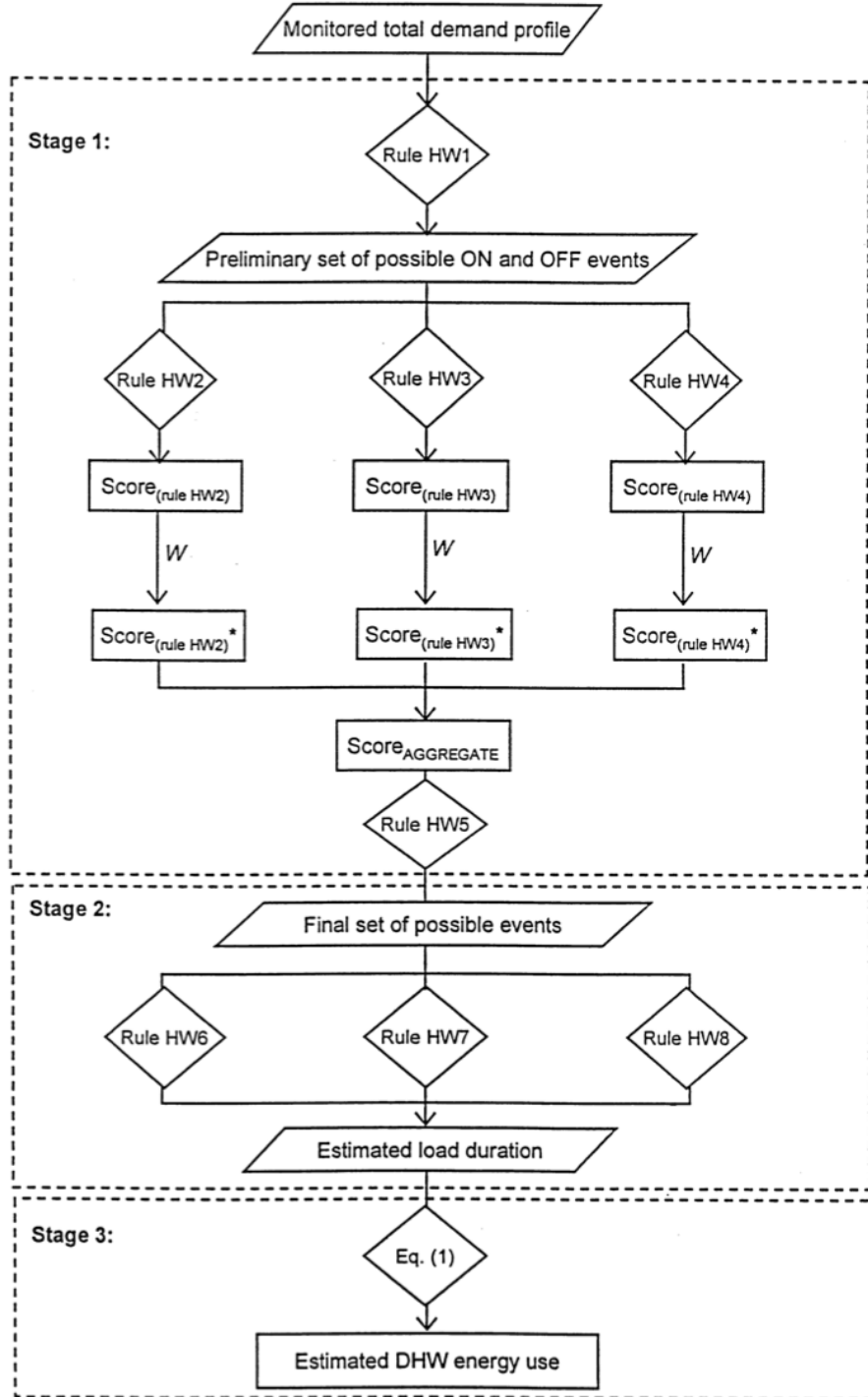


FIGURE 2.9: Flowchart for the pattern recognition algorithm [28]. Rule HW1 - the state change detection rule. Rule HW2 - the profile vector norm rule. Rule HW3 - the number of data points rule. Rule HW4 - the total demand rule. Rule HW5 - the minimum score rule. Rule HW6 - the highest scoring event rule. Rule HW7 - the minimum ON and OFF interval rule. Rule HW8 - the minimum total demand rule.

and some of them are non-intuitive and complicated. As illustrated in Figure 2.9, the flowchart of pattern recognition algorithm to detect and estimate the energy consumption of the Domestic Hot Water (DHW) heater comprises of three stages with many rules. The first stage is responsible for identifying the start and end events from the monitored aggregate power. The first rule, *state change detection* rule (HW1), is applied to detect a preliminary set of events based on the step-changes on the power draw. The three following rules, including *profile vector norm* rule (HW2), *number of data points* rule (HW3) and *total demand* rule (HW4), are then applied to evaluate each event and an aggregate score is finally used to confirm or refuse the occurrence of an event detected by the first rule through the *minimum score* rule (HW5). The remaining set of events are then sent to the second state to estimate the daily load duration of DHW heater, where three rules including *highest scoring event* rule (HW6), *minimum ON and OFF interval* rule (HW7) and *minimum total demand* rule (HW8) try to match the variation in the total power with the characteristic increase of each appliance obtained from the training period. Once all events are determined, the daily total power consumption of the DHW heater can be estimated by applying the Equation (2.13), as follows:

$$W = \sum S_i \times \Delta t \times w \quad [\text{Wh/day}], \quad (2.13)$$

where S_i is 1 if the appliance is estimated as ON at time instant i and 0 if OFF, Δt is the sampling interval equal to 16s and w is the average power demand of the appliance.

With the refrigerator type, the algorithm is similar except for the decision rules of the first stage, where the *total demand* rule is replaced by the *baseboard false event* rule to minimize the ambiguity with the baseboard, which has the similar first or second time-step. Although this method achieved the accuracy about 80%, their are some drawbacks preventing it from widely implemented such as excessive training or complex rule system. On the other hand, the appliances are assumed not to simultaneously change their states.

Also want to regconize the large loads, Prudenzi [29] applies the Artificial Neural Network (ANN) to determine the time of use of water heater (group H) and washing machine/dish washer (group W). Before going to the identification procedure, as shown in Figure 2.10, the available daily data is sampled every 15 minutes and divided into six 8-hour segments: 0.00 - 8.00, 4.00 - 12.00, 8.00 - 16.00, 12.00 - 20.00, 16.00 - 24.00, 20.00 - 4.00. In the first state (*pre-processing* state) the segments containing at least one energy usage of the

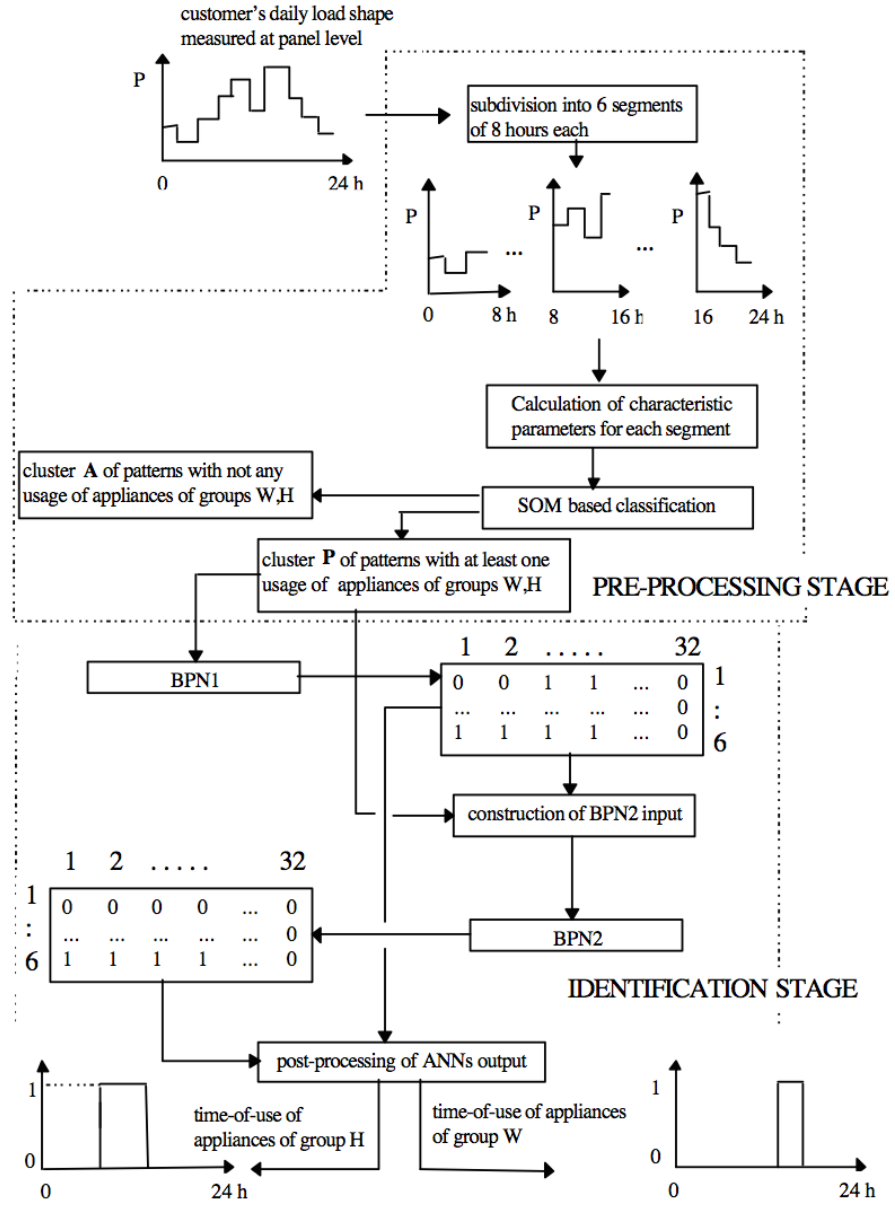


FIGURE 2.10: Simplified schematic of the ANN-based appliance identification [29].

appliances of both group W and H are determined and classified to cluster P, which will be processed in the next stage. Meanwhile, the segments without any usage of energy will be rejected. Self-Organizing Map (SOM) is applied in this stage to process three following principle parameters:

- x_{max} : maximum power of each segment;
- x_{avg} : average power of each segment;

- Δx_{max} : maximum of power change in each segment calculated by:

$$\Delta x_{max} = \max |x_{i+1} - x_i|_{i=1,\dots,n}.$$

In the second stage (*identification* stage), two supervised neuron nets (BPN1 and BPN2) with 32 inputs, 24 hidden neurons and 32 outputs are applied to process the data in cluster P. BPN1 receives the patterns from the first state, detects the energy usage of any appliance of group H, W and fills in the 6×32 -cell output table, each row of which corresponds to a segment and each column to one time instant. Because the appliances of group H, W consume a larger power in comparison with other appliances in home, they can be easily detected by analyzing the average power. The output of BPN1 is filtered by multiplying the output of the first stage and sent to BPN2. In this neuron net, the patterns of group H will be discriminated from ones of group W by applying the moving average operation. The output of BPN2 is also a 6×32 -cell table, however, contains only the information of the water heater. Combining the outputs of ANN, including the outputs of BPN1 and BPN2, the time-of-use of each group will be determined in the post-processing stage. Although this research only consideres the energy usage of such two groups as water heater and washing machine/dish washer, it contributes a new procedure for pattern identification by applying the ANN technique. With the accuracy over 90%, this method can be extended to more type of appliances with more complex scenarios.

Beside ANN, Hidden Markov Model (HMM) is also applied to find the states of the appliances in NILM [30, 31]. The state of each appliance can be considered as a hidden variable, while the observations relate to the aggregate power consumption measured by the smart meter at the main entry of electricity. In [30], the aggregate power consumption x as well as the difference on the power between two consecutive time slices, denoted as $y = x_i - x_{i-1}$, are considered as the observations of the so-called difference HMM, as represented in Figure 2.11, to find the state s of the appliances. The dependencies among the variables of each appliance in this model are defined by a three parameters learned from the training dataset:

$$\theta^{(i)} = \{\pi^{(i)}, A^{(i)}, \phi^{(i)}\}, \quad (2.14)$$

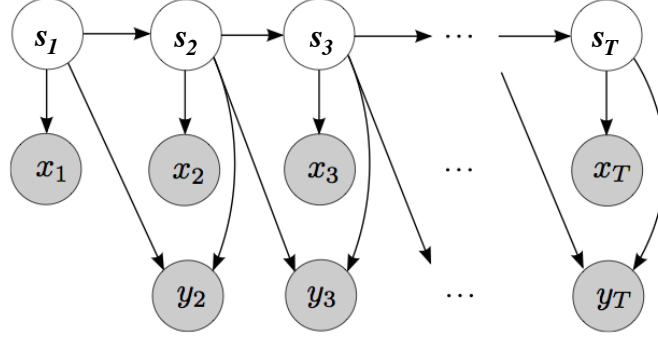


FIGURE 2.11: Difference HMM. Shaded nodes represent observations and unshaded nodes represent hidden variables [30].

where (i) denotes the i -th appliance and will be omitted for conciseness in the rest of this section, π is the probability of the initial state:

$$p(s_1 = k) = \pi_k; \quad (2.15)$$

A is the transition probability matrix from state a at time $t - 1$ to state b at time t :

$$p(s_t = b | s_{t-1} = a) = A_{a,b}; \quad (2.16)$$

and ϕ is the emission probability generated by an appliance state, which is assumed to have a Gaussian distribution:

$$w_t | s_t, \phi \sim N(\mu_{s_t}, \sigma_{s_t}^2), \quad (2.17)$$

with μ and σ^2 be the mean and variance, respectively. The distribution of difference observation y can be derived as follows:

$$y_t | s_t, s_{t-1}, \phi \sim N(\mu_{s_t} - \mu_{s_{t-1}}, \sigma_{s_t}^2 + \sigma_{s_{t-1}}^2). \quad (2.18)$$

In addition, a constraint needs to be imposed is that an appliance is only ON if the aggregate power is larger than its demand, or by the following cumulative distribution function:

$$\begin{aligned} P(w_{s_t} \leq x_t | s_t, \phi) &= \int_{-\infty}^{x_t} N(\mu_{s_t}, \sigma_{s_t}^2) dw \\ &= \frac{1}{2} \left[1 + \text{erf}\left(\frac{x_t - \mu_{s_t}}{\sigma_{s_t} \sqrt{2}}\right) \right]. \end{aligned} \quad (2.19)$$

The state of each individual appliance is determined by applying the extension of the Viterbi algorithm through two steps. In the first step, a filter is applied to suppress the observations whose joint probability does not exceed the predefined threshold C :

$$t \in S = \begin{cases} \text{true} & \text{if } \max_{s_{t-1}, s_t} (p(y_t|s_{t-1}, s_t, \theta)) \geq C \\ \text{false} & \text{otherwise.} \end{cases} \quad (2.20)$$

where S is the set of filtered observations. The second step evaluates the joint probability of all sequences x, y, s to identify the appliances:

$$\begin{aligned} p(x, y, s|\theta) = & p(s_1|\pi) \prod_{t=2}^T p(s_t|s_{t-1}, A) \\ & \prod_{t=1}^T P(w_{s_t} \leq x_t|s_t, \phi) \prod_{t \in S} p(y_t|s_t, s_{t-1}, \phi) \end{aligned} \quad (2.21)$$

Meanwhile, in [31], only aggregate power consumption is considered as observation instead of combining with the difference on the power between two consecutive time instants. In this research, most on-durations of home appliances are modeled as following the gamma distribution with a couple of parameters $\kappa^{(i)}, \theta^{(i)}$ for each appliance i . Besides, some additional features such as time of day, day of week and environment information from the sensors are also taken into account. Considering K additional conditions in HMM creates a variant of HMM called Conditional Factorial Hidden Semi-Markov Model (CFHSMM) and illustrated by the graphical model in Figure 2.12.

The hidden variables of this model can be found by applying the Maximum Likelihood Estimation (MLE) after training the set of parameters λ :

$$s^* = \arg \max_s P(X, s|\lambda), \quad (2.22)$$

where the joint probability $P(X, s|\lambda)$ is the product of the initial probability $\psi_{in}(X, s|\lambda)$, the emission probability $\psi_e(X, s|\lambda)$, and the transition probability $\psi_t(X, s|\lambda)$:

$$P(X, s|\lambda) = \psi_{in}(X, s|\lambda) \times \psi_e(X, s|\lambda) \times \psi_t(X, s|\lambda). \quad (2.23)$$

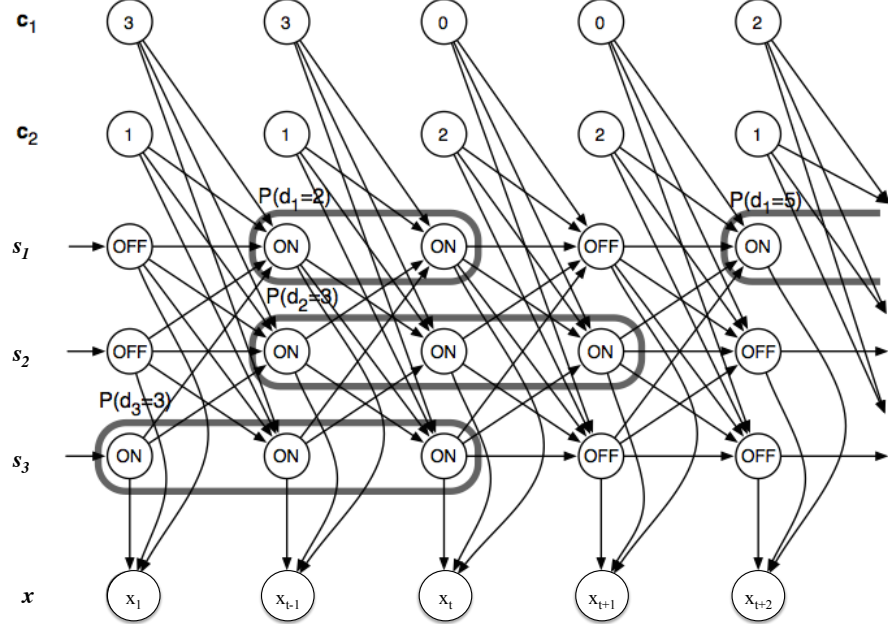


FIGURE 2.12: The graphical representation of CFHSMM with c_1, c_2 be the additional conditions [31].

The initial probability and emission probability are calculated as follows:

$$\psi_{in}(X, s|\lambda) = \prod_{i=1}^N \pi_{s_1^{(i)}}^{(i)}, \quad (2.24)$$

$$\psi_e(X, s|\lambda) = \prod_{t=1}^T b_{s_t}(x_t), \quad (2.25)$$

where denoting $\pi_{s_1^{(i)}}^{(i)} = P(s_1^{(i)})$ as the initial probability of appliance i and $b_{s_t}(x_t)$ as the emission probability of s_t if the observation is x_t , with $s_t = \{s_t^{(1)}, \dots, s_t^{(N)}\}$; while the transition probability is as follows:

$$\begin{aligned} \psi_t(X, s|\lambda) &= \prod_{i=1}^N \prod_{t:s_t^{(i)}=0} \left(\left(\prod_{j=1}^N m_{s_{t+1}^{(i)} j s_t^{(j)}}^{(i)} \right) \left(\prod_{j=1}^K f_{s_{t+1}^{(i)} j c_t^{(j)}}^{(i)} \right) \right) \\ &\quad \prod_{t:s_t^{(i)}=1} \left(\left(\prod_{j=1: i \neq j}^N m_{s_{t+1}^{(i)} j s_t^{(j)}}^{(i)} \right) \left(\prod_{j=1}^K f_{s_{t+1}^{(i)} j c_t^{(j)}}^{(i)} \right) \right), \\ &\quad \prod_{t:s_t^{(i)}=1, s_{t-1}^{(i)}=0} P(d = l_t^{(i)} | \kappa^{(i)}, \theta^{(i)}) \end{aligned} \quad (2.26)$$

where $m_{s_{t+1}^{(i)} k s_t^{(j)}}^{(i)} = P(s_t^{(j)} | s_{t+1}^{(i)})$ is the conditional probability for appliance j of state $s_t^{(j)}$, $f_{s_{t+1}^{(i)} j c_t^{(j)}}^{(i)} = P(c_t^{(j)} | s_{t+1}^{(i)})$ is the conditional probability for feature j of value l and $l_t^{(i)}$ is the length of the on-duration of appliance i beginning from time t .

Constructing the problem in the context of NILM as an HMM can give an effective state determination approach for low frequency power measurement. It helps to improve the accuracy and open many perspectives to develop in future work. The accuracy of this method varies depending on the tested house, type and number of appliances. However, this approach exists some limitations such as excessive training period to consider the distribution of the variables as well as complexity computation.

2.3 Non-Intrusive Load Monitoring: Microscopic

In many cases, the low frequency hardware based NILM algorithm cannot discern the state of some appliances having the same power characteristics. Besides, if an appliance consumes a variable energy over time, the steady state does not exist and the detection algorithm cannot accurately operate. Therefore, other algorithms based on a higher sampling frequency need to be studied. The target of the researches using high sampling rate data can focus on the harmonics and especially, the transient phase, which contains much information about the appliances. The cost, however, will also increase along with the augment of the frequency.

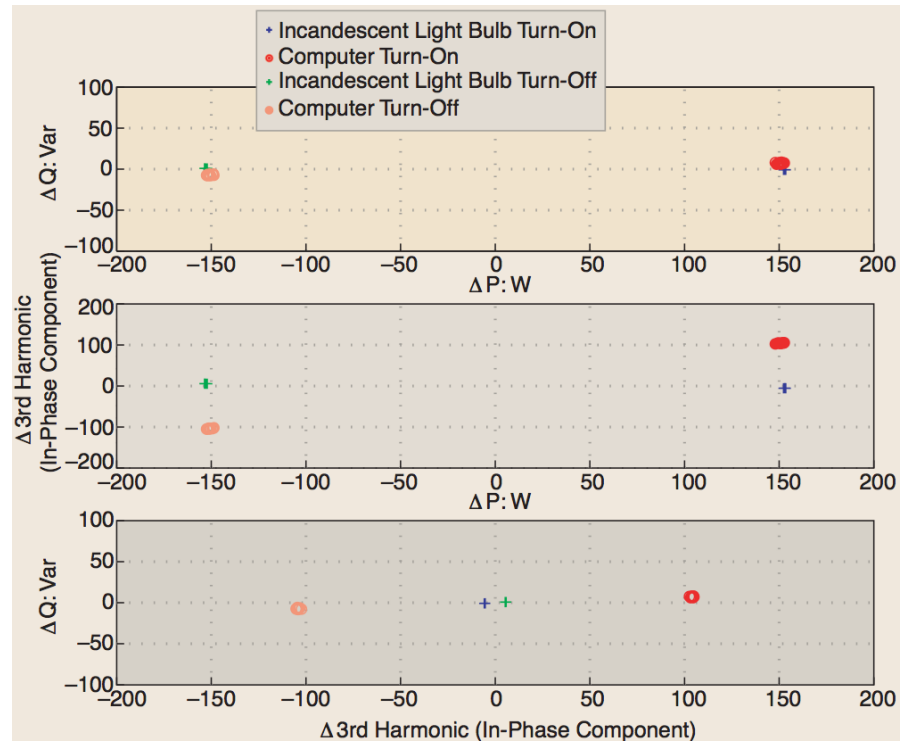


FIGURE 2.13: The computer and incandescent light bulb cannot be discriminated by the real and reactive power but can be distinguished by the third harmonic [32].

In [32], the indistinguishable problem of the appliances consuming the same power level in [20] is solved by using the third harmonic of the phase-locked short-time Fourier transform of current waveforms collected at 8000 Hz and higher sampling rates. As shown in Figure 2.13, an incandescent light bulb and a computer cannot be discriminated if using only the first harmonics, i.e. real and reactive power, but can be distinguishable by analyzing the third harmonics. In some circumstances, analyzing higher harmonics, e.g. 7th, 9th, etc., is necessary. Additionally, as presented in [32], the operating appliances can also be detected by matching the events on the transient phase of the aggregate power draw with the predefined signatures obtained from the training period. For example, the turn-on transient phases related to a computer and an incandescent lamp are distinguishable because heating the lamp filament is different from charging the power supply capacitors of the computer. Furthermore, transient-based recognition also allows near-real-time identification of energy consumers, particularly switch-on events.

However, detecting complete transient shapes is sometimes a waste of memory and not necessary. That is the reason why in [22, 33], the authors introduce a new time pattern called *v-shape*, which is the periods containing the significant changes during the transient phase. Figure 2.14 shows an example of the *v-shapes* in the transient phase of an induction motor. The principle of *v-shape*-based appliance identification is to search for the precise time pattern of *v-shape* and compare with the patterns in the library.

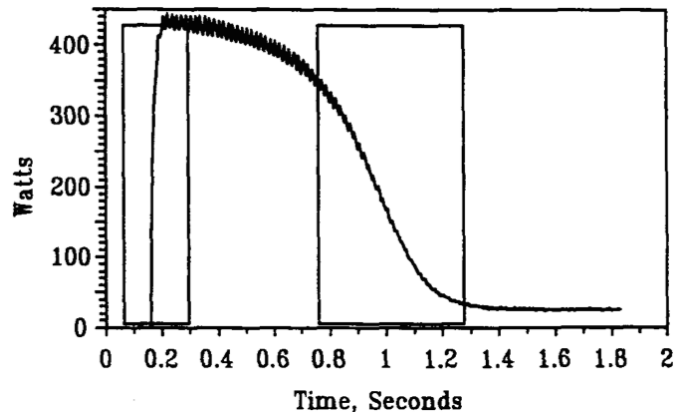


FIGURE 2.14: *v-shapes* on the transient of an induction motor [33].

A limitation of the transient-based NILM is that it cannot detect exactly the appliances if they are simultaneously switched ON or OFF. Therefore, in [34], Fast Fourier Transform (FFT) is applied to analyze the harmonics of the incoming current waveform. Both real and imaginary of the harmonics are the inputs of an ANN, in which the number of inputs

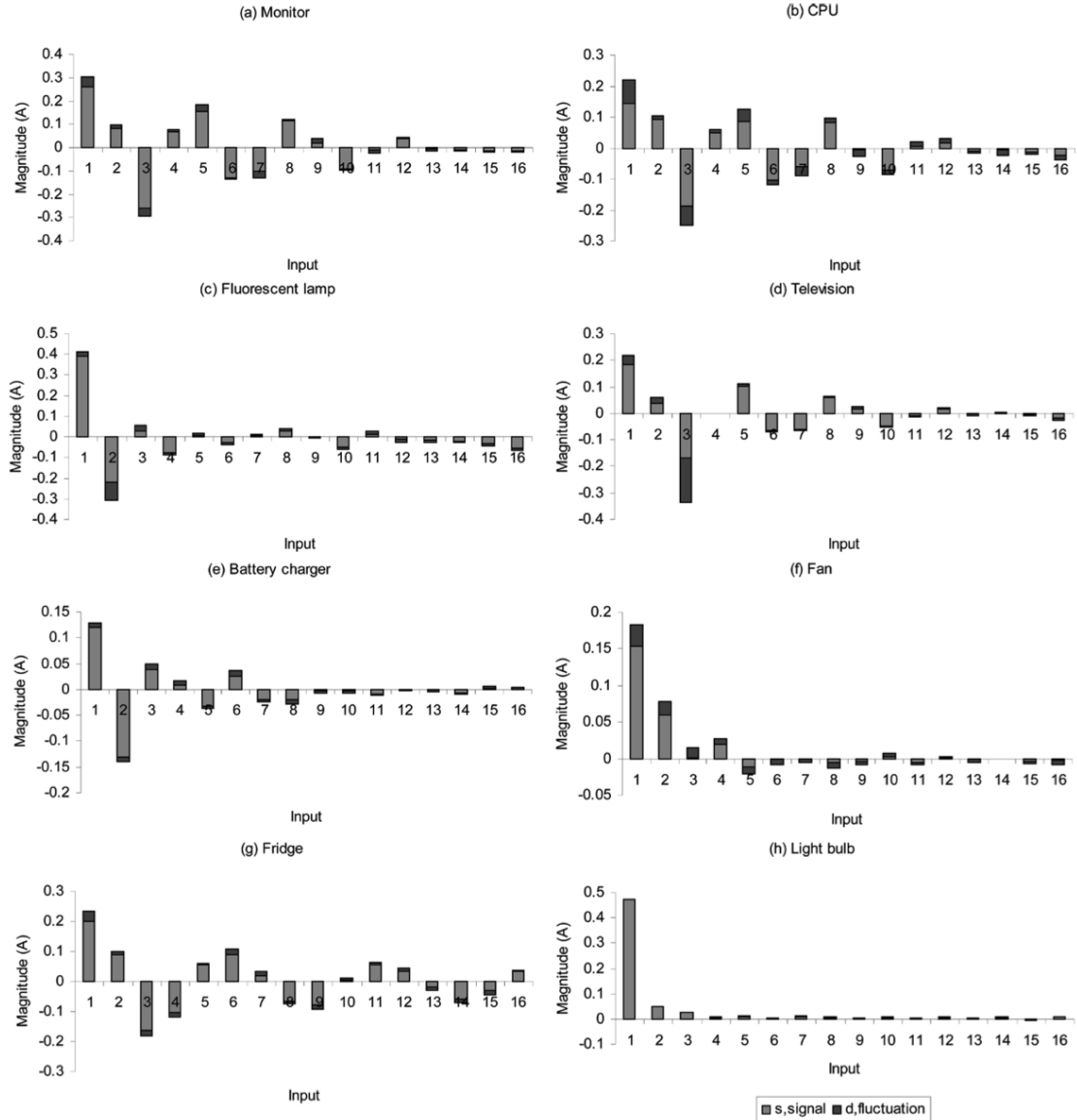


FIGURE 2.15: Harmonic signatures of some devices [34].

depends on the effectiveness of additional harmonics, while the number of outputs relates to the number of classes, or number of known appliances. The mean value and standard deviation of the harmonics of some typical devices are represented in Figure 2.15 and the identification system is shown in Figure 2.16.

In another research, the authors of [35] introduce a new approach to identify the running devices by detecting the noise created on the monitored power line, based on a high frequency hardware and 2048-point FFT. Every house or building has some appliances running on background and the power waveform of the background noise is saved on the memory. Whenever a new appliance operates, a noise is created on the background and the respective running appliance can be identified by analyzing the frequency components

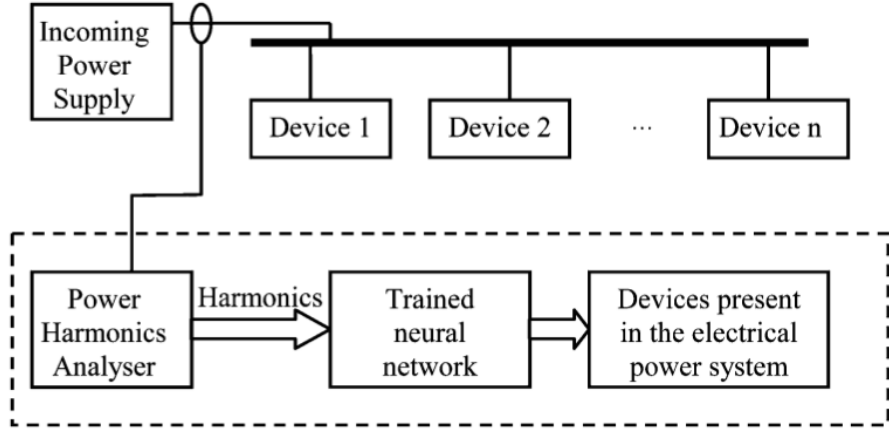


FIGURE 2.16: Device identification system model [34].

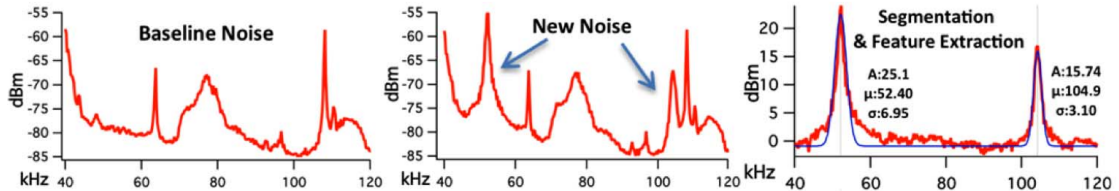


FIGURE 2.17: New noise feature detected and extracted from the background noise [35].

of the measured signal. For example, Figure 2.17 shows the new signal appearing on the background noise and its extracted frequency components.

Bibliography

- [1] <https://www.smartgrid.gov/>.
- [2] S. Galli, A. Scaglione, and Zhifang Wang. Power line communications and the smart grid. In *Smart Grid Communications (SmartGridComm), 2010 First IEEE International Conference on*, pages 303–308, Oct 2010. doi: 10.1109/SMARTGRID.2010.5622060.
- [3] S. Galli, A. Scaglione, and Zhifang Wang. For the grid and through the grid: The role of power line communications in the smart grid. *Proceedings of the IEEE*, 99(6):998–1027, June 2011. ISSN 0018-9219. doi: 10.1109/JPROC.2011.2109670.
- [4] V.C. Gungor, D. Sahin, T. Kocak, S. Ergut, C. Buccella, C. Cecati, and G.P. Hancke. Smart grid technologies: Communication technologies and standards. *Industrial Informatics, IEEE Transactions on*, 7(4):529–539, Nov 2011. ISSN 1551-3203. doi: 10.1109/TII.2011.2166794.
- [5] L.T. Berger, A. Schwager, and J.J. Escudero-Garzas. Power line communications for smart grid applications. *Journal of Electrical and Computer Engineering*, 2013, 2013. URL <http://dx.doi.org/10.1155/2013/712376>.
- [6] <http://fr.nec.com/>.
- [7] Yuvraj Agarwal, Rajesh Gupta, Thomas Weng, and Bharathan Balaji, Bharathan andx Dutta. Duty-cycling buildings aggressively: The next frontier in HVAC control. In *IEEE/ACM Information Processor in Sensor Networks*, pages 246–257, Chicago, IL, USA, April 2011.
- [8] T. Weng and Y. Agarwal. From buildings to smart buildings-sensing and actuation to improve energy efficiency. *Design Test of Computers, IEEE*, 29(4):36–44, 2012. ISSN 0740-7475. doi: 10.1109/MDT.2012.2211855.

- [9] Yuvraj Agarwal, Bharathan Balaji, Rajesh Gupta, Jacob Lyles, Michael Wei, and Thomas Weng. Occupancy-driven energy management for smart building automation. In *Proceedings of the 2nd ACM Workshop on Embedded Sensing Systems for Energy-Efficiency in Building*, pages 1–6, New York, NY, USA, 2010.
- [10] Jiakang Lu, Tamim Sookoor, Vijay Srinivasan, Ge Gao, Brian Holben, John Stankovic, Eric Field, and Kamin Whitehouse. The smart thermostat: Using occupancy sensors to save energy in homes. In *Proceedings of the 8th ACM Conference on Embedded Networked Sensor Systems*, SenSys ’10, pages 211–224, New York, NY, USA, 2010. ACM. ISBN 978-1-4503-0344-6. doi: 10.1145/1869983.1870005.
- [11] Dong Chen, Sean Barker, Adarsh Subbaswamy, David Irwin, and Prashant Shenoy. Non-intrusive occupancy monitoring using smart meters. In *Proceedings of the 5th ACM Workshop on Embedded Sensing Systems for Energy-Efficiency in Building*, pages 1–8, New York, NY, USA, 2013.
- [12] Shengwei Wang, John Burnett, and Hoishing Chong. Experimental validation of co₂-based occupancy detection for demand-controlled ventilation. *Indoor and Built Environment*, 8(6):377–391, 1999. doi: 10.1177/1420326X9900800605. URL <http://ibe.sagepub.com/content/8/6/377.abstract>.
- [13] Younghun Kim, Thomas Schmid, Zainul M. Charbiwala, and Mani B. Srivastava. Viridiscope: Design and implementation of a fine grained power monitoring system for homes. In *Proc. Ubicomp09*, pages 245–254, 2009.
- [14] Anthony Rowe, Mario Berges, and Raj Rajkumar. Contactless sensing of appliance state transitions through variations in electromagnetic fields. In *Proceedings of the 2Nd ACM Workshop on Embedded Sensing Systems for Energy-Efficiency in Building*, BuildSys ’10, pages 19–24, New York, NY, USA, 2010. ACM. ISBN 978-1-4503-0458-0. doi: 10.1145/1878431.1878437. URL <http://doi.acm.org/10.1145/1878431.1878437>.
- [15] Deokwoo Jung and Andreas Savvides. Estimating building consumption breakdowns using on/off state sensing and incremental sub-meter deployment. In *Proceedings of the 8th ACM Conference on Embedded Networked Sensor Systems*, SenSys ’10, pages 225–238, New York, NY, USA, 2010. ACM. ISBN 978-1-4503-0344-6. doi: 10.1145/1869983.1870006. URL <http://doi.acm.org/10.1145/1869983.1870006>.

- [16] Deokwoo Jung and Andreas Savvides. Theory and algorithm of estimating energy consumption breakdowns using on/off state sensing. *ACM Trans. Sen. Netw.*, 11(1):5:1–5:36, sep 2014. ISSN 1550-4859. doi: 10.1145/2630880. URL <http://doi.acm.org/10.1145/2630880>.
- [17] Christian Beckel, Wilhelm Kleiminger, Thorsten Staake, and Silvia Santini. Improving device-level electricity consumption breakdowns in private households using on/off events. *SIGBED Rev.*, 9(3):32–38, July 2012. ISSN 1551-3688. doi: 10.1145/2367580.2367586. URL <http://doi.acm.org/10.1145/2367580.2367586>.
- [18] J. Zico Kolter and Matthew J. Johnson. REDD: A public data set for energy disaggregation research. In *In SustKDD*, 2011.
- [19] J. Z. Kolter, Siddharth Batra, and Andrew Y. Ng. Energy disaggregation via discriminative sparse coding. In J.D. Lafferty, C.K.I. Williams, J. Shawe-Taylor, R.S. Zemel, and A. Culotta, editors, *Advances in Neural Information Processing Systems 23*, pages 1153–1161. Curran Associates, Inc., 2010. URL <http://papers.nips.cc/paper/4054-energy-disaggregation-via-discriminative-sparse-coding.pdf>.
- [20] G.W. Hart. Nonintrusive appliance load monitoring. *Proceedings of the IEEE*, 80(12):1870–1891, Dec 1992. ISSN 0018-9219. doi: 10.1109/5.192069.
- [21] M. Zeifman and K. Roth. Nonintrusive appliance load monitoring: Review and outlook. *IEEE Transactions on Consumer Electronics*, 57(1):76–84, 2011. ISSN 0098-3063. doi: 10.1109/TCE.2011.5735484.
- [22] Leslie K. Norford and Steven B. Leeb. Non-intrusive electrical load monitoring in commercial buildings based on steady-state and transient load-detection algorithms. *Energy and Buildings*, 24(1):51 – 64, 1996. ISSN 0378-7788. doi: [http://dx.doi.org/10.1016/0378-7788\(95\)00958-2](http://dx.doi.org/10.1016/0378-7788(95)00958-2).
- [23] A.I. Cole and A. Albicki. Data extraction for effective non-intrusive identification of residential power loads. In *Instrumentation and Measurement Technology Conference, 1998. IMTC/98. Conference Proceedings. IEEE*, volume 2, pages 812–815 vol.2, May 1998. doi: 10.1109/IMTC.1998.676838.
- [24] Jing Liao, Georgia Elafoudi, Lina Stankovic, and Vladimir Stankovic. Non-intrusive appliance load monitoring using low-resolution smart meter data. In *In Proceedings*

- of the 5th Annual IEEE International Conference on Smart Grid Communications*, pages 541–546, Venice, Italy, 2014.
- [25] D.L. Olson and D. Delen. *Advanced Data Mining Techniques*. Springer, 2008.
- [26] N. Batra, H. Dutta, and A. Singh. Indic: Improved non-intrusive load monitoring using load division and calibration. In *Machine Learning and Applications (ICMLA), 2013 12th International Conference on*, volume 1, pages 79–84, Dec 2013. doi: 10.1109/ICMLA.2013.21.
- [27] M.L. Marceau and R. Zmeureanu. Nonintrusive load disaggregation computer program to estimate the energy consumption of major end uses in residential buildings. *Energy Conversion and Management*, 41(13):1389 – 1403, 2000. ISSN 0196-8904. doi: [http://dx.doi.org/10.1016/S0196-8904\(99\)00173-9](http://dx.doi.org/10.1016/S0196-8904(99)00173-9).
- [28] Linda Farinaccio and Radu Zmeureanu. Using a pattern recognition approach to disaggregate the total electricity consumption in a house into the major end-uses. *Energy and Buildings*, 30(3):245 – 259, 1999. ISSN 0378-7788. doi: [http://dx.doi.org/10.1016/S0378-7788\(99\)00007-9](http://dx.doi.org/10.1016/S0378-7788(99)00007-9). URL <http://www.sciencedirect.com/science/article/pii/S0378778899000079>.
- [29] A. Prudenzi. A neuron nets based procedure for identifying domestic appliances pattern-of-use from energy recordings at meter panel. In *Power Engineering Society Winter Meeting, 2002. IEEE*, volume 2, pages 941–946 vol.2, 2002. doi: 10.1109/PESW.2002.985144.
- [30] Oliver Parson, Siddhartha Ghosh, Mark Weal, and Alex Rogers. Non-intrusive load monitoring using prior models of general appliance types. In *1st International Workshop on Non-Intrusive Load Monitoring*, pages 356–362, Pittsburgh, PA, USA, 2012.
- [31] Hyungsul Kim, Manish Marwah, Martin Arlitt, Geoff Lyon, and Jiawei Han. Unsupervised disaggregation of low frequency power measurements. In *11th International Conference on Data Mining*, pages 747–758, Arizona, USA, 2011.
- [32] C. Laughman, Kwangduk Lee, R. Cox, S. Shaw, S. Leeb, L. Norford, and P. Armstrong. Power signature analysis. *Power and Energy Magazine, IEEE*, 1(2):56–63, Mar 2003. ISSN 1540-7977. doi: 10.1109/MPAE.2003.1192027.

- [33] S.B. Leeb, S.R. Shaw, and Jr. Kirtley, J.L. Transient event detection in spectral envelope estimates for nonintrusive load monitoring. *Power Delivery, IEEE Transactions on*, 10(3):1200–1210, Jul 1995. ISSN 0885-8977. doi: 10.1109/61.400897.
- [34] D. Srinivasan, W. S. Ng, and A.C. Liew. Neural-network-based signature recognition for harmonic source identification. *Power Delivery, IEEE Transactions on*, 21(1):398–405, Jan 2006. ISSN 0885-8977. doi: 10.1109/TPWRD.2005.852370.
- [35] Sidhant Gupta, Matthew S. Reynolds, and Shwetak N. Patel. Electrisense: Single-point sensing using emi for electrical event detection and classification in the home. In *In Proceedings of the 12th ACM International Conference on Ubiquitous Computing*, pages 139–148, Copenhagen, Denmark, 2010.